Calculation of magnetic field noise from high-permeability magnetic shields and conducting objects with simple geometry

S.-K. Lee and M. V. Romalis

Related Articles

Enhancement of glass-forming ability of Fe-based bulk metallic glasses with high saturation magnetic flux density
AIP Advances 2, 022169 (2012)

Magnetoelectric relaxation in rhombohedral LiNbO3-CoFe2O4
Appl. Phys. Lett. 100, 262907 (2012)

Broadband probing magnetization dynamics of the coupled vortex state permalloy layers in nanopillars
Appl. Phys. Lett. 100, 262406 (2012)

The effects of group-I elements co-doping with Mn in ZnO dilute magnetic semiconductor
J. Appl. Phys. 111, 123524 (2012)

Magnetic hysteresis of an artificial square ice studied by in-plane Bragg x-ray resonant magnetic scattering
AIP Advances 2, 022163 (2012)

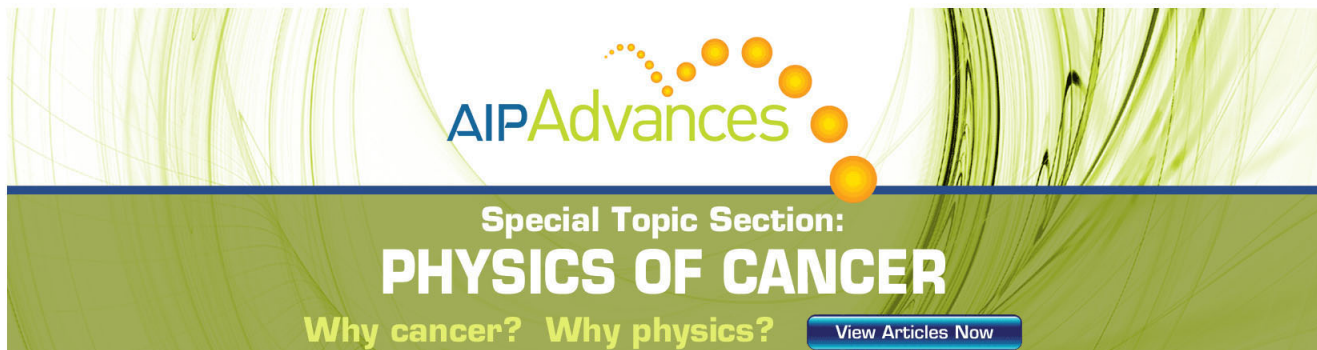## Additional information on J. Appl. Phys.

Journal Homepage: http://jap.aip.org/

Journal Information: http://jap.aip.org/about/about_the_journal

Top downloads: http://jap.aip.org/features/most_downloaded

Information for Authors: http://jap.aip.org/authors

Calculation of magnetic field noise from high-permeability magnetic shields and conducting objects with simple geometry

S.-K. Lee[a)] and M. V. Romalis

Physics Department, Princeton University, Princeton, New Jersey 08544, USA

High-permeability magnetic shields generate magnetic field noise that can limit the sensitivity of modern precision measurements. We show that calculations based on the fluctuation-dissipation theorem allow quantitative evaluation of magnetic field noise, either from current or magnetization fluctuations, inside enclosures made of high-permeability materials. Explicit analytical formulas for the noise are derived for a few axially symmetric geometries, which are compared with results of numerical finite element analysis. Comparison is made between noises caused by current and magnetization fluctuations inside a high-permeability shield and also between current-fluctuation-induced noises inside magnetic and nonmagnetic conducting shells. A simple model is suggested to predict power-law decay of noise spectra beyond a quasi-static regime. Our results can be used to assess noise from existing shields and to guide design of new shields for precision measurements. © *2008 American Institute of Physics.* [DOI: 10.1063/1.2885711]

I. INTRODUCTION

Passive magnetic shields are frequently used in precision measurements to create a region in space that is magnetically isolated from the surroundings.[1] A few layers of nested shells made of high-permeability metals, such as mu-metal, routinely provide in table-top experiments a quasi-static shielding factor in excess of 10^4. Such a shield, on the other hand, generates thermal magnetic field noise that often exceeds the intrinsic noise of modern high-sensitivity detectors such as superconducting quantum interference devices (SQUIDs) and high-density alkali atomic magnetometers.[2]

Magnetic field noise generated by thermal motion of electrons (Johnson noise current) in metals has been much studied in the past in the context of applications of SQUID magnetometers,[3,4] and more recently as a source of decoherence in atoms trapped near a metallic surface.[5] A majority of these works were devoted to low frequency noise from Johnson noise current in nonmagnetic metals. A few authors also considered noise from high-permeability metals of flat geometry. The calculations presented in these works, however, were not particularly amenable to extension to other geometries, such as those of cylindrical shields often used in table-top experiments. Nenonen *et al.*, for example, used calculation of noise from an infinite slab to estimate noise inside a cubic magnetically shielded room for biomagnetic measurements.[6] As shown below, the validity of such extrapolation is not immediately clear, given the image effect of high-permeability plates. Lack of explicit formulas and qualitative scaling relations for magnetic field noise from high-permeability shields have caused some confusion about the contribution of such noise in certain experiments. (See discussions in Refs. 7 and 8.)

Among different strategies that have been demonstrated to calculate magnetic field noise,[3,4,9] a particularly versatile

method is the one based on the generalized Nyquist relation by Callen and Welton,[4,10] which later led to the fluctuation-dissipation theorem. Here the noise from a dissipative material is obtained from calculation of power loss incurred in the material by a driving magnetic field. Sidles *et al.*, for example, presented a comprehensive analysis of the spectrum of magnetic field noise from magnetic and nonmagnetic infinite slabs with a finite thickness using this principle.[11]

A particularly useful feature of the power-loss-based noise calculation is that it allows calculation of noise from multiple physical origins, including Johnson noise current in metals and domain fluctuations in magnetic materials. The noise of the latter kind in ferromagnets, which can be associated with magnetic hysteresis loss, was previously studied for toroidal transformer cores where field lines were confined in the core material.[12] In a recent work[13] Kornack *et al.* measured magnetic field noise in the interior of a ferrite enclosure with an atomic magnetometer, which was consistent with predictions based on numerical calculation of power loss in the ferrite. The same paper also presented results of analytical calculations of the noise inside an infinitely long, high-permeability cylindrical tube.

In this work we show how similar calculations can be performed for other geometries with cylindrical symmetry, and derive a general relationship between magnetic field noises from current and magnetization fluctuations in shields with such geometries. For metallic shields, we show that the Johnson-current-induced noise is either suppressed or amplified, depending on the shape of the shield, due to a high permeability. This partly explains previous confusion about noise contributed by magnetic metals. Analytical calculations leading to our key results were confirmed by numerical calculations on representative geometries using commercial finite element analysis software. In order to explain frequency dependence of noise from metallic and magnetic plates reported in the literature, we propose a simple model which correctly predicts observed power-law decays in noise spec-

---

a)Electronic mail: lsk@princeton.edu.

tra. We also present in Appendix B analytical calculations of noise from nonmagnetic conducting objects that can model other common experimental parts used in precision measurements.

II. PRINCIPLES

The principle of calculating magnetic field noise from energy dissipation in the source material has been demonstrated by several authors. For example, see Refs. 4, 5, and 11. The argument is summarized as follows. If at a point $\vec{r}$ there is a fluctuation of magnetic field along a direction $\hat{n}$, with power spectral density $S_B(f)$, an N-turn pickup coil located at $\vec{r}$ directed along $\hat{n}$ will develop a fluctuating voltage, according to the Faraday's law, with power spectral density

$$S_V(f) = A^2 N^2 \omega^2 S_B(f). \tag{1}$$

Here $\omega = 2\pi f$ and A is the area of the pickup coil, assumed to be small so that the field is uniform over the area. We further assume that the coil is purely inductive, for example by making it superconducting, so that in the absence of an external material (noise source) there is no voltage fluctuation due to conventional Nyquist noise, $S_{V,\text{coil}} = 4kTR_{\text{coil}} = 0$. Now assume that we take the pickup coil and the material responsible for the noise as a single effective electronic element, whose small-excitation response is characterized by an impedance Z. The fluctuation-dissipation theorem applied to this system states that the voltage fluctuation at the terminals of the pickup coil is related to the real part of Z, $\text{Re}[Z(f)] \equiv R_{\text{eff}}$, by

$$S_V(f) = 4kTR_{\text{eff}}(f). \tag{2}$$

Here the system is assumed to be at thermal equilibrium at temperature T, k is the Boltzmann constant, and the effective resistance R_{eff} is obtained from the time-averaged power dissipation in the system

$$P(f) = \frac{1}{2}I^2 R_{\text{eff}}(f) \tag{3}$$

incurred by an oscillating current $I(t) = I \sin \omega t$ flowing in the pickup coil whose amplitude I is small so that the response is linear. In the absence of the resistance of the pickup coil itself, the power dissipation is entirely due to the loss in the material driven electromagnetically by the current $I(t)$. From Eqs. (1)–(3) this power determines the magnetic field noise by

$$\delta B(f) \equiv \sqrt{S_B(f)} = \frac{\sqrt{4kT}\sqrt{2P(f)}}{ANI\omega}. \tag{4}$$

Since the power P scales quadratically with the driving dipole $p \equiv ANI$ in the linear response regime, the above equation is independent of the size and driving current of the pickup coil. The usefulness of this expression lies in the fact that, in most cases, calculation of power loss is much easier than that of magnetic field noise, the latter requiring an incoherent sum of vectorial contributions from many fluctuation modes inside the source material.

For high-permeability metals and ceramics used for magnetic shields the primary sources of power loss at low frequencies ($\lesssim 1$ MHz) are eddy current loss P_{eddy}

$= \int_V \frac{1}{2} \sigma E^2 \, dv$ and hysteresis loss $P_{\text{hyst}} = \int_V \frac{1}{2} \omega \mu'' H^2 \, dv.$[14,15] Here σ is the conductivity, μ'' is the imaginary part of the permeability $\mu = \mu' - i\mu''$, and the integrals are over the volume of the material in which oscillating electric and magnetic fields of amplitude E and H, respectively, are induced by $I(t)$.

For a given driving dipole strength p, the eddy current $j = \sigma E$ is proportional to the frequency ω, therefore P_{eddy} leads to a frequency independent (white) noise according to Eq. (4), to the extent that σ is frequency independent. On the other hand, P_{hyst}, assuming frequency-independent μ, leads to a noise with $1/f$ power spectrum, which is indeed observed in experiments with ferromagnetic transformer cores.[12] In the following sections we will denote the noises associated with P_{eddy} and P_{hyst} by δB_{curr} and δB_{magn}, respectively.

We emphasize that by applying the Nyquist relation to noise calculation, we assume that the noise generating medium is linear. Whereas ferromagnets are in general not linear, many materials, including mu-metal and Mn-Zn ferrite, used for magnetic shields and transformers are soft by requirement. For these materials, the energy needed for domain wall movement and reorientation is much less than kT, and the response of magnetization to harmonic driving field is well represented by a (frequency-dependent) complex permeability. Previous experimental measurements of the magnetic noise generated by soft ferromagnetic toroidal transformers[12] and a Mn-Zn ferrite enclosure[13] have shown good agreement with calculations based on the Nyquist relation. In addition to the steady-state thermal noise considered here, if a ferromagnet is subjected to a time-dependent driving magnetic field, sudden, steplike movements of domain walls also produce Barkhausen noise.[16] Since this is not a typical experimental situation in precision measurements, such noise is not considered in this paper.

III. POWER LOSS CALCULATION FOR HIGH-PERMEABILITY SHIELDS WITH CYLINDRICAL SYMMETRY

In this section we calculate power dissipation in high-permeability shields with cylindrical symmetry when the driving dipole is on and along the axis of the shield. See Fig. 1(a) for a representative geometry. We restrict ourselves to a quasi-static regime where the magnetic field amplitude inside the shield material is given by its dc value, ignoring perturbation due to induced (eddy) currents, which is proportional to the frequency. The power dissipation when the dipole is at other locations and along other directions can be calculated numerically with, for instance, a three-dimensional finite element analysis software commonly used for power loss calculations in transformer cores.

Figure 1(a) also shows several magnetic field lines, calculated numerically, in the ρ-z plane around the shield generated by a current loop modeling a driving dipole. Two features are noticeable. First, the field lines entering the shield are very nearly normal to the surface, reflecting the well-known boundary condition involving a high-permeability material. Second, most of the field lines reaching the shield are subsequently confined within the thickness of the shell,
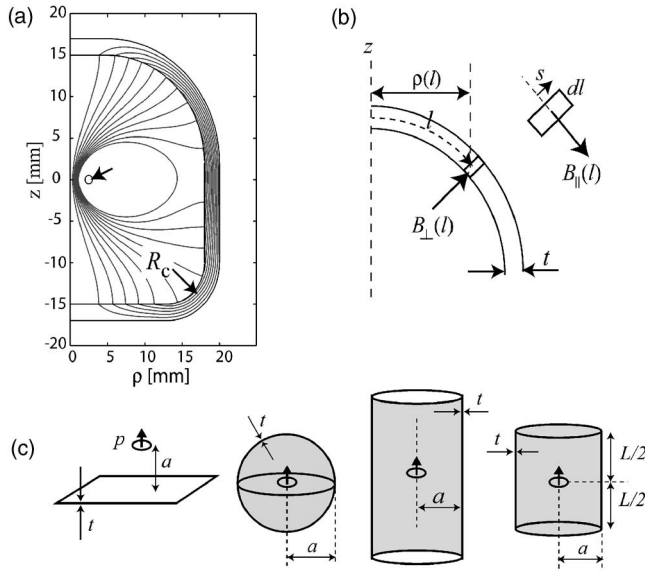
FIG. 1. (a) Magnetic field lines inside a high-permeability ($\mu_r = 1000$) shield with cylindrical symmetry. Mirror symmetry with respect to a transverse plane is not assumed. The field is generated by a current loop of radius 2.5 mm centered on the z axis, carrying 1 A dc; the small circle indicated by the arrow shows the cross section of the wire. The field lines closest to the wire are not shown. The 11 field lines that are shown enclose magnetic flux of $n\Delta\Phi$, $n = 1, 2, \ldots, 11$, where $\Delta\Phi = 10^{-10}$ Wb. (b) Cross section of the shield in the ρ-z plane. (c) Four geometries considered in the power loss calculation: infinite plate, sphere, infinite cylinder, and finite closed cylinder. The cylinders and the sphere are hollow shells of thickness t.

running nearly parallel to the profile of the shield in the ρ-z plane. This, combined with the condition $\nabla \times \vec{B} = 0$, requires that the field lines are nearly uniformly spread within the thickness of the shield. For a shield surface with radius of curvature (in the ρ-z plane) R_c, it can be shown that the variation of the field strength across the thickness t of the shield is $\delta B_\parallel / B_\parallel \approx t/R_c$, where $B_\parallel$ is the field component parallel to the shield in the ρ-z plane. The condition for the field confinement can be estimated, from dimensional consideration, to be $\mu_r t/a \gg 1$, where μ_r is the relative permeability, and a is the characteristic distance between the driving dipole and the shield surface.[17] Since the same factor $\mu_r t/a$ also determines the shielding factor,[1] we can assume this condition is satisfied if the shell is to function as a magnetic shield in the first place. In summary, we assume the following for our calculations: (1) $\mu_r \gg 1$ so that the normal entrance boundary condition is satisfied. (2) $\mu_r t/a \gg 1$ so that most of the field lines, once entering the shield material, are confined within the thickness of the shield. (3) $t/R_c \ll 1$ for most part of the shield so that the confined field amplitude is uniform in the direction normal to the shield surface.[18]

A. Eddy-current loss

Suppose that the driving dipole is oscillating sinusoidally at a frequency ω, $\vec{p}(t) = p\hat{z}\sin\omega t$. We want to calculate, to the lowest order in ω, the eddy current in the shield which is symmetric around the z axis. We define the position of an arbitrary point in the shield in the ρ-z plane by coordinate (l, s) as shown in Fig. 1(b). Here l defines a position in the midplane of the shield by measuring its distance from the z

axis along the cross section of the shield. The coordinate s represents the normal distance of a point from the midplane, $-t/2 \le s \le t/2$. Since we are interested in a thin-walled shell, we ignore the variation of the radial coordinate ρ on s: $\rho(l, s) \approx \rho(l, s = 0) \equiv \rho(l)$. Our assumptions in the preceding paragraph imply that the magnetic field within the shield material is parallel to the line defining the l coordinate, and its amplitude $B_\parallel = B_\parallel(l)$ depends only on l. Finally, we define $B_\perp(l)$ as the amplitude of the magnetic field entering the inner surface of the shield at $(l, s = -t/2)$.

In three dimensions, a point (l, s) corresponds to a ring, and we define $\Phi(l, s)$ as the amplitude of the flux generated by the driving dipole $\vec{p}(t)$ that threads the ring. Then the amplitude of the eddy current flowing along the ring is

$$j_\phi = \sigma E_\phi = \sigma \cdot \omega \cdot \Phi(l, s)/2\pi\rho(l). \qquad (5)$$

If all the field lines are confined within the shield, a ring on the outside surface of the shield has no net flux in it: $\Phi(l, s = t/2) = 0$. For all other s, $\nabla \cdot \vec{B} = 0$ dictates that

$$\Phi(l, s) = 2\pi\rho(l)\left(\frac{t}{2} - s\right)B_\parallel(l). \qquad (6)$$

From Eqs. (5) and (6) the eddy-current loss is

$$
\begin{aligned}
P_{\text{eddy}} &= \int_0^{l_{\max}} \int_{-t/2}^{t/2} \frac{1}{2}\sigma E_\phi^2(l,s) 2\pi\rho(l)\, ds\, dl \\
&= \int_0^{l_{\max}} \int_{-t/2}^{t/2} \frac{1}{2}\sigma\omega^2\left(\frac{t}{2}-s\right)^2 B_\parallel^2(l) 2\pi\rho(l)\, ds\, dl \\
&= \pi\sigma\omega^2 \int_0^{l_{\max}} B_\parallel^2(l)\rho(l)\, dl \int_{-t/2}^{t/2}\left(\frac{t}{2}-s\right)^2 ds \\
&= \frac{1}{3}\pi\sigma\omega^2 t\,\beta,
\end{aligned}
$$

where the configuration integral β, having a dimension of flux squared, is

$$\beta = \int_0^{l_{\max}} t^2 B_\parallel^2(l)\rho(l)\, dl. \qquad (7)$$

This expression can be reduced to a form more useful in practical calculations by expressing $B_\parallel(l)$ in terms of $B_\perp(l)$. From $\nabla \cdot \vec{B} = 0$ it follows that $t B_\parallel(l)\rho(l) = \int_0^l B_\perp(l')\rho(l')dl'$. Therefore,

$$\beta = \int_0^{l_{\max}} \left[\int_0^l B_\perp(l')\rho(l')dl'\right]^2 \frac{1}{\rho(l)} dl. \qquad (8)$$

B. Hysteresis loss

The hysteresis loss arises from a phase delay in the magnetic response of a material to the applied oscillating magnetic field. For most soft magnetic materials used for magnetic shields, this delay is small at frequencies below ~ 1 MHz. In the following we assume that the shield has a constant permeability throughout its volume with $\mu'' \ll \mu' \approx \mu_r\mu_0$. The expression for P_{hyst}, to the first order in μ'', can then be obtained as follows:

$$P_{\text{hyst}} = \int_V \frac{1}{2}\, \omega\, \mu''H^2\, dv$$

$$= \int_0^{l_{\max}} \int_{-t/2}^{t/2} \frac{1}{2}\, \omega\, \frac{\mu''}{\mu'^2} B_{\parallel}^2(l) 2\,\pi\,\rho\,(l)ds\, dl$$

$$= \pi\,\omega\, \frac{\mu''}{\mu'^2}\frac{1}{t}\,\beta\,.$$

Therefore, both P_{eddy} and P_{hyst} are proportional to β. It follows that the ratio between magnetization- and current-induced noises in a cylindrically symmetric shell measured on and along the axis is

$$\frac{\delta B_{\text{magn}}}{\delta B_{\text{curr}}} = \left(\frac{P_{\text{hyst}}}{P_{\text{eddy}}}\right)^{1/2}$$

$$= \left(\frac{3\mu''}{\sigma\,\omega\,\mu'^2 t^2}\right)^{1/2} = \sqrt{\frac{3}{2}}\frac{\delta_{\text{skin}}}{t}\sqrt{\tan\,\delta_{\text{loss}}}, \qquad (9)$$

where we used the definitions of skin depth $\delta_{\text{skin}} = 1/\sqrt{\pi\mu'\,\sigma f}$ and loss tangent $\tan\,\delta_{\text{loss}} = \mu''/\mu'$. Therefore δB_{magn} becomes relatively important when the skin depth is greater than $\sim t/\sqrt{\tan\,\delta_{\text{loss}}}$. This is equivalent to $f \lesssim f_{\text{magn}}$ where

$$f_{\text{magn}} = 3\tan\,\delta_{\text{loss}}/2\pi\mu_r\mu_0\sigma t^2. \qquad (10)$$

C. Field noise equations

In this section we list explicit formulas for the magnetic field noise for shields of simple geometries shown in Fig. 1(c), namely an infinite plate, an infinite cylindrical shell, a spherical shell, and a finite-length, closed cylindrical shell. From the considerations in the previous sections, the on-axis magnetic field noise inside a cylindrically symmetric, thin-walled shield can be calculated analytically from the knowledge of $B_{\perp}(l)$. Calculation of $B_{\perp}$ is analogous to that of an electric field on the inside surface of a conducting shell induced by an on-axis electric dipole. Such calculation is most easily performed by the method of an image in the case of an infinite plate and a sphere. For a cylinder, Smythe[19] gives a series expansion solution that can be readily adopted for calculation of $B_{\perp}$.

1. Infinite plate

The midplane of the plate is the x-y plane, and the driving dipole $p\hat{z}$ is at $z=a$ on the z axis. l is measured from the origin. Due to the image effect of a high-permeability plate, $B_{\perp}(l)$ is twice as large as the normal component of a dipolar field expected in free space. Explicitly,

$$B_{\perp}(l) = \frac{\mu_0 p}{2\,\pi}\frac{-1+3\cos^2\theta}{(a^2+l^2)^{3/2}},$$

where $\cos\,\theta = a/\sqrt{a^2+l^2}$. This gives

$$\delta B_{\text{curr}} = \frac{1}{\sqrt{6\pi}}\frac{\mu_0\sqrt{kT\,\sigma\,t}}{a}. \qquad (11)$$

2. Spherical shell

For a driving dipole $p\hat{z}$ at the center of a sphere with radius a, the image "dipole" consists of two "monopoles" $\pm 2ap/d^2$ positioned at $z=\mp 2a^2/d$, in the limit $d\to 0$. The resulting surface normal field is

$$B_{\perp}(l) = \frac{3\mu_0 p}{4\,\pi\,a^3}\cos\frac{l}{a},$$

where l runs from the north pole to the south pole of the sphere, $0<l<\pi a$, and

$$\delta B_{\text{curr}} = \frac{1}{\sqrt{2\,\pi}}\frac{\mu_0\sqrt{kT\,\sigma\,t}}{a}. \qquad (12)$$

3. Infinite cylindrical shell

Smythe[19] gives the electrostatic potential $V(\rho,z)$ inside an infinitely long conducting cylindrical tube, symmetric around the z axis, due to a point charge q inside the tube. When q is at the origin and the tube is grounded, it is

$$V(\rho,z) = \frac{q}{2\pi\epsilon_0 a}\sum_\alpha e^{-\alpha|z|/a}\frac{J_0(\alpha\rho/a)}{\alpha J_1^2(\alpha)},$$

where ϵ_0 is the permittivity of vacuum, $J_n(x)$ is the Bessel function of order n, and the summation is over the zeros of J_0; $J_0(\alpha)=0$. From this expression, the surface normal (radial) magnetic field at $\rho=a$ due to a magnetic dipole $p\hat{z}$ at the origin can be obtained as

$$B_{\perp}(z) = \mu_0\epsilon_0 d\frac{\partial}{\partial z}\frac{\partial}{\partial\rho}V(\rho,z)\Big|_{\rho=a,qd=p}$$

$$= \text{sign}(z)\frac{\mu_0 p}{2\,\pi\,a^3}\sum_\alpha\frac{\alpha e^{-\alpha|z|/a}}{J_1(\alpha)}.$$

As a result,

$$\delta B_{\text{curr}} = \frac{\mu_0\sqrt{kT\,\sigma\,t}}{a}\sqrt{\frac{2}{3\,\pi}}G,$$

$$G = \int_{-\infty}^{\infty} dz'\left(\sum_\alpha\frac{e^{-\alpha|z'|}}{J_1(\alpha)}\right)^2 \approx 0.435. \qquad (13)$$

4. Closed cylindrical shell of finite length

Reference 19 also gives the electrostatic potential when the conducting cylinder is closed at, say, $z=\pm L/2$, by conducting plates. For a charge q at $(\rho=0, z=z_1)$, the potential at a point $(\rho<a, z>z_1)$ is

$$V(\rho,z;z_1) = \frac{q}{\pi\epsilon_0 a}\sum_\alpha\frac{\sinh\,\alpha\left(\frac{L}{2a}+\frac{z_1}{a}\right)\sinh\,\alpha\left(\frac{L}{2a}-\frac{z}{a}\right)}{\sinh\,\alpha\frac{L}{a}}$$

$$\times\frac{J_0(\alpha\rho/a)}{\alpha J_1^2(\alpha)}.$$

If the conducting shell is replaced by a high-permeability magnetic shield and a magnetic dipole $p\hat{z}$ replaces q, the normal magnetic field at the top plate is

$$B_\perp^{top} = B_z(\rho, z = L/2) = -\mu_0 \epsilon_0 d \frac{\partial}{\partial z} \frac{\partial}{\partial z_1} V(\rho, z; z_1)|_{z=L/2, qd=p}.$$

Similarly the normal field on the side wall at $z > z_1$ is

$$B_\perp^{side} = B_\rho(\rho = a, z) = -\mu_0 \epsilon_0 d \frac{\partial}{\partial \rho} \frac{\partial}{\partial z_1} V(\rho, z; z_1)|_{\rho=a, qd=p}.$$

For simplicity, in the following we consider only the case when $p\hat{z}$ is located at the origin, $z_1 = 0$, which gives the noise at the center of the shield. Then, by symmetry, calculation of β requires an integral over only the upper half of the cylinder. The integral path consists of two portions: the top plate where l runs along the line $(0 < \rho < a, z = L/2)$ and the upper half of the side wall where l runs along the line $(\rho = a, L/2 > z > 0)$.

Explicitly,

$$\frac{1}{2}\beta = \int_0^a \frac{1}{\rho} d\rho \left[\int_0^\rho B_\perp^{top}(\rho')\rho' \, d\rho' \right]^2$$
$$+ \int_0^{L/2} \frac{1}{a} dz \left[\int_0^a B_\perp^{top}(\rho')\rho' \, d\rho' \right.$$
$$\left. + \int_z^{L/2} B_\perp^{side}(z')a \, dz' \right]^2.$$

The first term can be calculated using Bessel function identities $\int_0^u u' J_0(u') du' = u J_1(u)$ and $\int_0^1 dx x J_1(\alpha x) J_1(\alpha' x) = \frac{1}{2} J_1^2(\alpha)\delta_{\alpha\alpha'}$. This turns out to be $(\mu_0 p/2\pi)^2 (1/2a^2) F_1(L/a)$, where

$$F_1(x) = \sum_\alpha \frac{1}{\sinh^2 \frac{\alpha x}{2}} \cdot \frac{1}{J_1^2(\alpha)}. \tag{14}$$

The second term is more tedious, but can be reduced to $(\mu_0 p/2\pi)^2 (1/a^2) F_2(L/a)$ with[20]

$$F_2(x) = \int_0^{1/2} dx' x \left[\sum_\alpha \frac{1}{J_1(\alpha)} \cdot \frac{\cosh \alpha x x'}{\sinh \frac{\alpha x}{2}} \right]^2. \tag{15}$$

Finally, the field noise is

$$\delta B_{curr} = \frac{\mu_0 \sqrt{kT\sigma t}}{a} \sqrt{\frac{2}{3\pi}} G,$$

$$G = F_1(L/a) + 2F_2(L/a). \tag{16}$$

Numerical evaluation of the above equation shows that $G = 0.657, 0.460, 0.438$ for aspect ratios $L/2a = 1, 1.5, 2$, respectively. Thus the noise from a closed cylindrical shield with aspect ratio of 2 already approaches that of an infinitely long shield within 0.5%.

IV. COMPARISON WITH NOISE FROM NONMAGNETIC CONDUCTING SHELLS

An interesting question is how the magnetic field noise in a high-permeability shield compares with that in a nonmagnetic shell with the same geometry and conductivity. As indicated in Ref. 4, calculation of low-frequency eddy current loss in an axially symmetric, nonmagnetic conductor driven by an axial dipole $\vec{p} = p\hat{z}\sin\omega t$ is relatively simple,

because the amplitude of the induced electric field is proportional to the magnetostatic vector potential A_ϕ (in Coulomb gauge) due to a dipole in vacuum. For an axial dipole $p\hat{z}$ at the origin,

$$A_\phi(\rho, z) = \frac{\mu_0 p}{4\pi} \frac{\rho}{(\rho^2 + z^2)^{3/2}}$$

and

$$P_{eddy} = \frac{1}{2}\sigma\omega^2 \int_V A_\phi^2 \, dv,$$

where V is the volume of the conductor.

Equations for the quasi-static field noise associated with this loss are listed in Table I for the geometries considered in the previous section. For the cases of an infinite plate, a sphere, and a long cylinder, it is found that the current-induced noise inside a high-permeability shell is not much different from that inside a nonmagnetic shell. The difference can be either positive (infinite plate) or negative (sphere and cylinder). Qualitatively, one can think of two competing effects, namely self-shielding and image effects, due to the high permeability of the material. In a long tube, the field generated by a noise current at the end of the tube is self-shielded as it propagates inward. On the other hand, the field generated by a current loop on the surface of an infinite plate is amplified because of an image current adding field in the same direction.

A dramatic illustration of the latter effect is found in the case of field noise in between two infinite plates, with thickness t, separated by L. When the plates are nonmagnetic, the total quasi-static power loss induced by an axial driving dipole half-way between the plates is simply twice that induced in a single plate. In the limit $\mu_r t/L \to \infty$, however, it can be shown that the power loss and therefore the noise logarithmically diverges. This is because the noise current in either plate generates an infinite series of image currents, and when all the current modes are considered their contributions do not converge. This effect can be appreciated when we examine the noise inside a finite, closed cylinder in the limit of a low aspect ratio $(L/2a \ll 1)$. In Table I, inspection of the last equation in the rightmost column shows that as $L/2a \to 0$, δB for a nonmagnetic cylinder approaches $(1/\sqrt{4\pi})\mu_0\sqrt{kT\sigma t}\,(2/L)$. This is just a factor $\sqrt{2}$ larger than the noise from a single infinite plate (the first equation in the same column) measured at a distance $L/2$. For a high-permeability cylinder, numerical calculation of Eq. (16) with $L/2a = 0.5, 0.1, 0.05$ reveals that the corresponding factors referenced to the single plate case [Eq. (11)] are 1.66, 2.28, and 2.54, respectively, demonstrating clear departure from $\sqrt{2}$. It can be seen that the noise from a high-permeability structure cannot, in general, be obtained from the quadrature sum of the noise from its individual parts.

V. FREQUENCY DEPENDENCE

Here we consider how the noise δB_{curr} considered in Secs. III and IV rolls off at frequencies above the quasi-static regime. Previous theoretical and experimental works on noise from conducting plates and enclosures[21] reported ini-

TABLE I. Magnetic field noise from high-permeability and nonmagnetic plate and shells of conductivity σ. The geometries are shown in Fig. 1(c).

Geometry	Field noise due to Johnson noise current	
	High-permeability	Nonmagnetic
Infinite plate	$\delta B_{\mathrm{curr}} = \dfrac{1}{\sqrt{6\pi}}\dfrac{\mu_0\sqrt{kT\sigma t}}{a}$	$\delta B = \dfrac{1}{\sqrt{8\pi}}\dfrac{\mu_0\sqrt{kT\sigma t}}{a}$
Spherical shell	$\delta B_{\mathrm{curr}} = \dfrac{1}{\sqrt{2\pi}}\dfrac{\mu_0\sqrt{kT\sigma t}}{a}$	$\delta B = \sqrt{\dfrac{2}{3\pi}}\dfrac{\mu_0\sqrt{kT\sigma t}}{a}$
Infinite cylindrical shell	$\delta B_{\mathrm{curr}} = \sqrt{\dfrac{2G}{3\pi}}\dfrac{\mu_0\sqrt{kT\sigma t}}{a}$, $G \approx 0.435$	$\delta B = \sqrt{\dfrac{3}{16}}\dfrac{\mu_0\sqrt{kT\sigma t}}{a}$
Finite, closed cylindrical shell	Equations (14)–(16)	$\delta B = \sqrt{G}\dfrac{\mu_0\sqrt{kT\sigma t}}{a}$,
		$G = \dfrac{1}{8\pi}\left(\dfrac{3(L/2a)^5 + 5(L/2a)^3 + 2}{(L/2a)^2[1+(L/2a)^2]^2} + 3\tan^{-1}\dfrac{L}{2a}\right)$

tial roll-off given by $\delta B(f) \propto f^{-\gamma}$, where $\gamma \approx 1$ for nonmagnetic metals and $\gamma \approx 1/4$ for high-permeability metals. Below we provide qualitative explanation of such dependences by considering a simple model.

Suppose we measure noise from a large, thin plate with conductivity σ at a distance a along the direction perpendicular to the plate. We assume that σ is independent of frequency. The plate has a thickness $t \ll a$ and a lateral dimension much larger than a. It is reasonable to assume that the field noise mostly comes from fluctuating currents flowing in a series of concentric rings directly below the measurement point with radius on the order of a. Since these current paths are connected in parallel, we can assume that in fact the noise comes from current fluctuation in a single annular loop of mean radius $\approx a$ and width $\approx a$. The dc resistance of such a loop is $R_0 = 2\pi/\sigma t$, which gives conventional Johnson noise current $\delta I = \sqrt{4kT/R_0} \approx \sqrt{(2/\pi)kT\sigma t}$. The magnetic field noise arising from this current is indeed of the same order of magnitude as the noise calculated in the previous sections.

At high frequencies this current is suppressed in two ways. First, when $\delta_{\mathrm{skin}} < t$, the resistance increases by the skin depth effect to $R(f > f_{\mathrm{skin}}) \approx 2\pi/\sigma\delta_{\mathrm{skin}} \propto f^{1/2}$. The threshold frequency is

$$f_{\mathrm{skin}} = 1/\pi\mu_r\mu_0\sigma t^2. \tag{17}$$

Second, the self inductance L of the loop suppresses δI if $2\pi f L > R(f)$. Therefore the current noise should, in general, be written as open-loop voltage noise divided by total impedance,

$$\delta I = \frac{\sqrt{4kTR(f)}}{|R(f) + i2\pi fL|},$$

where $R(f)$ includes the skin depth effect. If the condition $2\pi fL > R(f)$ is reached at a frequency $f_{\mathrm{ind}} < f_{\mathrm{skin}}$, such frequency is obtained from $2\pi f_{\mathrm{ind}}L = R_0$, namely,

$$f_{\mathrm{ind}} = 1/\sigma tL = 1/C\mu_0\sigma ta, \tag{18}$$

where C is a constant of order unity. For a nonmagnetic plate, $f_{\mathrm{ind}}/f_{\mathrm{skin}} = (\pi/C)\mu_r t/a \ll 1$ and inductive screening indeed appears at a frequency far below that at which skin depth becomes important. The initial roll-off of the noise then occurs at $f \gtrsim f_{\mathrm{ind}}$, where the current noise scales with frequency as

$$\delta I \approx \frac{\sqrt{4kTR_0}}{2\pi fL} \propto f^{-1}, \quad f_{\mathrm{ind}} \lesssim f \lesssim f_{\mathrm{skin}}.$$

As f further increases beyond f_{skin}, the scaling changes to

$$\delta I \approx \frac{\sqrt{4kTR(f)}}{2\pi fL} \propto f^{-3/4}, \quad f_{\mathrm{skin}} \lesssim f.$$

On the other hand, for a high-permeability plate used for magnetic shields, skin depth effect appears at a frequency far below that for inductive screening, $f_{\mathrm{ind}}/f_{\mathrm{skin}} \gg 1$. Therefore the initial roll-off is expected to follow

$$\delta I \approx \frac{\sqrt{4kTR(f)}}{R(f)} \propto f^{-1/4}, \quad f_{\mathrm{skin}} \lesssim f \lesssim f'_{\mathrm{ind}}.$$

The frequency f'_{ind} at which inductive screening becomes important for a high-permeability plate is obtained from $2\pi f'_{\mathrm{ind}}L = R(f'_{\mathrm{ind}}) = 2\pi/\sigma\delta_{\mathrm{skin}}$, which reduces to

TABLE II. Frequency dependence of magnetic field noise induced by Johnson noise current in magnetic and nonmagnetic metallic plates.

Reference No.	Frequency dependence	Material	Method
11, Eq. (5)	$f^0 \rightarrow f^{-1} \rightarrow f^{-3/4}$	Non- or weakly magnetic slab	Calculated
3, Fig. 6	$f^0 \rightarrow f^{-1} \rightarrow f^{-3/4}$	Nonmagnetic slab	Calculated
7, Fig. 1	$f^0 \rightarrow f^{-1/4} \rightarrow f^{-3/4}$	High-permeability slab	Calculated
9, Fig. 2	$f^0 \rightarrow f^{-1}$	Nonmagnetic, thin sheet	Calculated
21, Fig. 2	$f^0 \rightarrow f^{-1/4}$	Mu-metal plate	Measured
	$f^0 \rightarrow f^{-1}$	Copper plate	Measured

$$f'_{\text{ind}} = (\pi/C^2)\mu_r/\mu_0 \sigma a^2. \qquad (19)$$

Beyond this frequency δI again scales as $f^{-3/4}$.

Table II summarizes the frequency dependence of the Johnson-current-induced magnetic field noise reported in five references. It is found that our simple model correctly predicts all the essential features of the frequency dependences found in these works. For nonmagnetic plates, the two threshold frequencies Eq. (17) and Eq. (18) agree, up to a numerical factor, with those obtained in Ref. 3[22] and Refs. 11.[23] For high-permeability plates, Table 1 of Ref. 7 also can be interpreted as giving the same threshold frequencies between different regimes, Eq. (17) and Eq. (19), obtained in this work.[24]

Finally, if we include the magnetization-fluctuation noise calculated in Sec. III B, the magnetic field noise from a high-permeability plate is expected to exhibit a rather complicated frequency dependence,

$$\delta B(f): f^{-1/2} \rightarrow f^0 \rightarrow f^{-1/4} \rightarrow f^{-3/4},$$

where the three threshold frequencies dividing different scaling regimes are given by Eqs. (10), (17), and (19), in the increasing order.

VI. NOISE REDUCTION BY DIFFERENTIAL MEASUREMENT

A common technique to reduce the effect of magnetic field noise from a distant source is to make a differential or gradiometric measurement. In the first-order differential measurement, one measures $B_{\text{diff}}(t) = B_1(t) - B_2(t)$, where B_1 and B_2 are the magnetic fields at two points separated by a baseline d. The fluctuation in this quantity $\delta B_{\text{diff}}(f)$ can be calculated following the same principles described in Sec. II, with a single pickup coil replaced by two coils connected in series so that the induced voltage is proportional to B_{diff}. Reduction of noise from a distant source now corresponds to reduction of power loss induced in the material when driven by this "gradiometric" coil, which appears as a quadrupole, rather than a dipole, seen from a distance $a \gg d$. If the two coils connected in series are identical, each represented by an oscillating dipole of amplitude p, then the resulting power loss P gives δB_{diff} through

$$\delta B_{\text{diff}}(f) = \frac{\sqrt{4kT}\sqrt{2P(f)}}{p\,\omega}.$$

In the limit $a \gg d$, P is proportional to the square of the driving quadrupole moment $p^2 d^2$. From dimensional consideration, therefore, δB_{diff} scales as (d/a).

Table III shows the results of analytical calculations of δB_{diff} for an infinite plate and an infinitely long cylindrical shell. Only the white noise associated with the eddy current loss is considered. The noise is calculated for an axial differential measurement along the symmetry axis, in the limit where the baseline is much smaller than the shortest distance a to the material. It is seen that in all cases the noise reduction factor is very nearly d/a.

VII. CONCLUSION

We have used the generalized Nyquist relation applied to electromagnetic power dissipation and magnetic field fluctuation to calculate magnetic field noise inside high-permeability magnetic shields. Analytical results for axially symmetric geometries show that the quasi-static field noise due to Johnson current noise in a metallic shell is slightly altered as the material gains high magnetic permeability. For magnetic shields with small electrical conductivity, $1/f$ noise from magnetization fluctuations becomes dominant over Johnson-current-induced noise below a threshold frequency proportional to its magnetic loss factor. Established numerical methods of finite-element analysis of electromagnetic power loss can be of great utility in calculating magnetic field noise spectrum from dissipative materials of complicated geometry. At relatively high frequencies, one could experimentally determine the power loss in dissipative materials using a pickup coil. This has an advantage that no prior knowledge of material parameters is necessary to predict the field noise. From Eqs. (3) and (4), it turns out that a 1 fT/Hz$^{1/2}$ noise at 1 kHz and at room temperature corresponds to an effective resistance of 10 mΩ in a 1000-turn driving coil of 5 cm diameter. This change in the resistive load is within the measurement range of modern impedance analyzers.

As reported earlier,[2] we find that quasi-static Johnson current noise in magnetic shields is significantly higher than intrinsic noise of modern magnetometers. Due to a small skin depth of high-permeability materials, however, the white noise range extends only to relatively low frequencies ($f_{\text{skin}} = 1-100$ Hz), beyond which the noise rolls off as $f^{-1/4}$, until self-induction effect further brings down the noise. This

TABLE III. Differential measurement noise from an infinite plate and a long cylindrical shell of conductivity σ. d indicates the separation of the two measurement points along the symmetry axis. δB_{single} in the last column is the magnetic field noise in nondifferential measurement taken from Table I.

Geometry	Material	δB_{diff}	$\delta B_{diff}/\delta B_{single}$
Infinite plate	High-permeability	$\dfrac{1}{\sqrt{4\pi}}\dfrac{\mu_0\sqrt{kT\sigma t}}{a}\dfrac{d}{a}$	$1.22\dfrac{d}{a}$
	Nonmagnetic	$\sqrt{\dfrac{3}{16\pi}}\dfrac{\mu_0\sqrt{kT\sigma t}}{a}d/a^{\,a}$	$1.22\dfrac{d}{a}$
Infinite cylindrical shell	High-permeability	$\sqrt{\dfrac{2G}{3\pi}}\dfrac{\mu_0\sqrt{kT\sigma t}}{a}\dfrac{d}{a},$	$1.19\dfrac{d}{a}$
		$G=\displaystyle\int_{-\infty}^{\infty}dz'\left(\sum_\alpha\dfrac{\alpha e^{-\alpha|z'|}}{J_1(\alpha)}\right)^2\approx 0.618$	
	Nonmagnetic	$\sqrt{\dfrac{45}{256}}\dfrac{\mu_0\sqrt{kT\sigma t}}{a}\dfrac{d}{a}$	$0.97\dfrac{d}{a}$

[a]This agrees with Eq. (43) of Ref. 3.

indicates that usual room-temperature mu-metal shields may be used without adding significant noise if the signal is modulated at relatively high frequencies. At low frequencies, most sensitive experiments would require a low-loss nonconducting magnetic materials, such as certain ferrites, as the innermost layer of a multi-layer shield, or differential field measurement with a short baseline. In practice, a combination of these techniques should be implemented to suppress shield-contributed noise to an insignificant level.

APPENDIX A: COMPARISON WITH NUMERICAL CALCULATIONS

Here we compare magnetic field noise predicted by analytical expressions in Table I with that obtained from numerical calculations of power loss for representative geometries. The calculation was performed by a finite element analysis software (Maxwell 2D, Ansoft) which determined electromagnetic fields in space on a mesh through iterative solution of the Maxwell's equations. The driving dipole was modeled as a small current loop on the symmetry axis. For P_{eddy}, the current oscillated at $f=0.01$ Hz. For P_{hyst}, a magnetostatic problem was solved with a static current in the coil, and the volume integral of H^2 in the material was calculated. Magnetic field noise was then obtained by Eq. (4). The errors due

to a nonzero radius of the loop were insignificant within the accuracy of the numerical calculations presented here.

Table IV shows magnetic field noise from high-permeability plate and shields. The loss tangent assumed is for illustration purpose only. It is seen that in all cases considered here, numerical and analytical results differ by less than 3%. The errors represent the accuracy of the assumptions made in magnetic field calculations in Sec. III.

Table V shows magnetic field noises from nonmagnetic plate and shells. These numbers can be used to estimate noise from nonmagnetic, metallic enclosures often used for radio-frequency shielding. The differences between analytical and numerical calculations, less than 1%, are consistent with the errors in the numerical calculations.

TABLE IV. Magnetic field noise calculated for mu-metal plate and enclosure with $\sigma=1.6\times10^6$ Ω^{-1} m^{-1}, $\mu_r=30\,000$, tan $\delta=0.04$. Geometrical parameters are $a=0.2$ m, $t=1$ mm, referenced to Fig. 1(c). Column 3 is calculated from equations in column 2 of Table I. Column 5 equals column 3 multiplied by 0.5628, from Eq. (9). Numerical calculation for an infinite plate was obtained by extrapolation of the results for finite-size plates.

Geometry	δB_{curr} (fT/Hz$^{1/2}$)		δB_{magn} (fT/Hz$^{1/2}$) at 1 Hz	
	Numerical	Analytical	Numerical	Analytical
Infinite plate	3.63	3.68	2.01	2.07
Spherical shell	6.38	6.38	3.57	3.59
Closed cylindrical shell				
$L/2a=0.5$	12.4	12.2	6.93	6.87
$L/2a=1.0$	6.01	5.97	3.33	3.36
$L/2a=1.5$	5.04	4.99	2.77	2.81
$L/2a=2.0$	4.92	4.87	2.70	2.74

TABLE V. Magnetic field noise from eddy current loss calculated in aluminum, $\sigma = 3.8 \times 10^7$ Ω^{-1} m^{-1}, $\mu_r = 1$. The geometries are the same as in Table IV.

Geometry	δB_{curr} (fT/Hz$^{1/2}$)	
	Numerical	Analytical
Infinite plate	15.4	15.5
Spherical shell	35.7	35.9
Closed cylindrical shell		
$L/2a = 0.5$	45.0	44.9
$L/2a = 1.0$	34.1	34.2
$L/2a = 1.5$	33.6	33.7
$L/2a = 2.0$	33.6	33.7

APPENDIX B: MAGNETIC FIELD NOISE FROM OTHER METALLIC OBJECTS

For the purpose of future reference, here we list equations for magnetic field noise resulting from Johnson noise currents in nonmagnetic, conducting objects with simple geometry. We only consider white noise in the low frequency limit. Table VI lists equations for a small solid sphere, thin planar films, and a long thin wire, as defined in Fig. 2. In the context of an atomic vapor-cell magnetometer, these objects can be associated with an alkali metal droplet, low-emissivity conductive coatings on a glass, and a heating wire, respectively. For problems with a cylindrical symmetry [Figs. 2(a) and 2(b)], the eddy-current loss induced by a driving dipole $\vec{p}(t) = \vec{p} \sin \omega t$ was calculated by the method outlined in Sec. IV. For others, the eddy current density can be calculated from the equations

$$\nabla \times \vec{j} = \sigma \nabla \times \vec{E} = -i\sigma\omega\vec{B},$$

$$\nabla \cdot \vec{j} = 0,$$

with the boundary condition that the normal component of $\vec{j}$ is zero on the surface (boundary) of the object. Here $\vec{B}$ is the amplitude of the oscillating magnetic field generated by $\vec{p}(t)$ in free space. For a thin film lying in the x-y plane, $\nabla \times \vec{j}$ is along the z axis and therefore only B_z contributes to the loss. The two-dimensional current distribution $\vec{j}(x,y) = (u(x,y), v(x,y))$ then satisfies

$$\frac{\partial u}{\partial y} - \frac{\partial v}{\partial x} = i \sigma \omega B_z, \qquad (B1)$$

TABLE VI. Magnetic field noise due to Johnson noise current in metallic objects with conductivity σ.

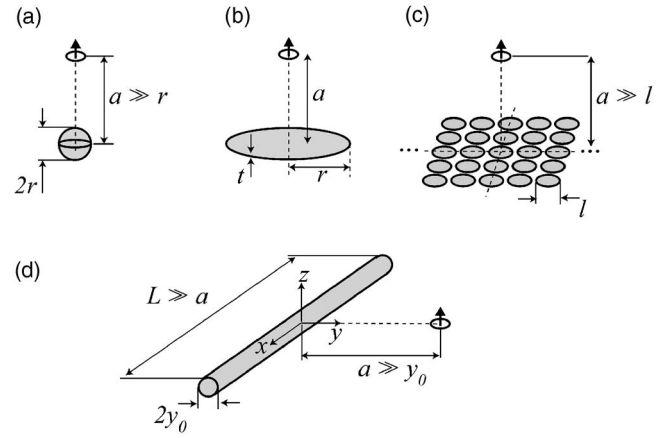| Geometry	δB	Figure No.
Small solid sphere	$\sqrt{4/15\pi}\,\mu_0\sqrt{kT\sigma}\,r^{5/2}a^{-3}$	2(a)
Thin film disk	$(1/\sqrt{8\pi})(\mu_0\sqrt{kT\sigma t}/a)(1/(1+a^2/r^2))$	2(b)
Infinite square array of small disks	$\sqrt{3/2048}\,\mu_0\sqrt{kT\sigma t}\,l/a^2$	2(c)
Circular cross-section wire	$\sqrt{3/128}\,\mu_0\sqrt{kT\sigma}\,y_0^2 a^{-5/2}$	2(d)

FIG. 2. Definition of geometries used to calculate magnetic field noise from (a) a small solid sphere, (b) a thin disk with arbitrary diameter, (c) a square array of small thin disks covering an infinite plane, and (d) a long, thin wire with a circular cross section. In (c), the small disks have thickness t, are close-packed, but are electrically isolated from each other.

$$\frac{\partial u}{\partial x} + \frac{\partial v}{\partial y} = 0. \qquad (B2)$$

When the film is divided into small patches whose lateral dimensions are much smaller than the distance to the dipole, the current distribution in each patch can be calculated assuming a constant B_z within the patch.

When the film is in the shape of a long, narrow strip, such as a long straight wire patterned on an insulating substrate, the noise measured along the z axis on a point in the x-y plane can be calculated by solving Eqs. (B1) and (B2) with the boundary condition $u(x = \pm L/2, y) = 0$, $v(x, y = \pm y_0) = 0$. Here the strip is assumed to occupy a region $-L/2 \le x \le L/2$, $-y_0 \le y \le y_0$ with $L \gg y_0$. The source term is given by $B_z(x,y) = (\mu_0 p / 4\pi a^3)(1 + x^2/a^2)^{-3/2}$, assuming the noise is measured at $(0, a, 0)$ and $a \gg y_0$. Equations (B1) and (B2) are then satisfied by

$$u(x,y) = \frac{\sigma\omega\mu_0 p}{\pi a L}\sum_n \cos k_n x \frac{\sinh k_n y}{\cosh k_n y_0} K_1(ak_n),$$

$$v(x,y) = \frac{\sigma\omega\mu_0 p}{\pi a L}\sum_n \sin k_n x \left(-1 + \frac{\cosh k_n y}{\cosh k_n y_0}\right) K_1(ak_n),$$

where K_1 is the modified Bessel function of order one and $k_n = (2n-1)\pi/L$, $n = 1, 2, \ldots$. The power loss in a strip with thickness dt, calculated in the limit $L/a \to \infty$, is

$$P(y_0)dt = \frac{dt}{\sigma}\int\int (u^2 + v^2)dx\,dy$$

$$= \frac{dt}{64\pi}\sigma(\omega\mu_0 p)^2 y_0^3 a^{-5}\left(1 - \frac{3}{8}\frac{y_0^2}{a^2} + \cdots\right).$$

For a wire with a circular cross section, the integral of the above equation over the profile (in the y-z plane) of the wire gives the total loss

$$P_{\text{wire}} = \int_{-y_0}^{y_0} P(\sqrt{y_0^2 - t^2})dt.$$

The corresponding magnetic field noise, in the leading order in y_0/a, is

$$\delta B = \sqrt{\frac{3}{128}}\mu_0 \sqrt{kT\,\sigma}\; y_0^2 a^{-5/2}.$$

For example, a long straight constantan wire with diameter $2y_0 = 1$ mm and $\sigma = 2 \times 10^6$ Ω^{-1} m^{-1} exhibits $\delta B = 0.433$ fT/Hz$^{1/2}$ at room temperature when measured at $a = 1$ cm in the direction perpendicular to both the wire and the normal direction to the wire.

[1] A. J. Mager, IEEE Trans. Magn. **6**, 67 (1970).

[2] J. C. Allred, R. N. Lyman, T. W. Kornack, and M. V. Romalis, Phys. Rev. Lett. **89**, 130801 (2002).

[3] T. Varpula and T. Poutanen, J. Appl. Phys. **55**, 4015 (1984).

[4] J. R. Clem, IEEE Trans. Magn. **23**, 1093 (1987).

[5] C. Henkel, Eur. Phys. J. D **35**, 59 (2005).

[6] J. Nenonen, J. Montonen, and T. Katila, Rev. Sci. Instrum. **67**, 2397 (1996).

[7] C. T. Munger, Jr., Phys. Rev. A **72**, 012506 (2005).

[8] D. Budker, D. Kimball, and D. DeMille, *Atomic Physics* (Oxford U. P., Oxford, 2004), Chap. 9.

[9] B. J. Roth, J. Appl. Phys. **83**, 635 (1998).

[10] H. B. Callen and T. A. Welton, Phys. Rev. **83**, 34 (1951).

[11] J. A. Sidles, J. L. Garbini, W. M. Dougherty, and S.-H. Chao, Proc. IEEE **91**, 799 (2003).

[12] G. Durin, P. Falferi, M. Cerdonio, G. A. Prodi, and S. Vitale, J. Appl. Phys. **73**, 5363 (1993).

[13] T. W. Kornack, S. J. Smullin, S.-K. Lee, and M. V. Romalis, Appl. Phys. Lett. **90**, 223501 (2007).

[14] D. Lin, P. Zhou, W. N. Fu, Z. Badics, and Z. J. Cendes, IEEE Trans. Magn. **40**, 1318 (2004).

[15] For low-conductivity soft ferromagnets, so-called excess or residual loss often dominates eddy current loss calculated with static bulk conductivity. In such cases we assume that the effect is included in an appropriately redefined $\sigma = \sigma(f)$.

[16] P. Mazzetti and G. Montalenti, J. Appl. Phys. **34**, 3223 (1963).

[17] This comes from the fact that for a given shield size and shape, the reluctance of the portion of the magnetic circuit that goes through the shield scales with the thickness and the permeability as $R_{\text{magn}} \propto 1/(\mu_r t)$. Therefore qualitative distribution of field lines around the shield should not change as μ_r and t vary while keeping their product constant. The other length scale relevant to the problem is a, which leads to the dimensionless parameter specified.

[18] Obviously this does not hold at the corners of a closed cylindrical shield. However, numerical finite-element calculations in Appendix A indicate that errors in noise due to these localized points are at most on the order of 1%.

[19] W. R. Smythe, *Static and Dynamic Electricity* (McGraw-Hill, New York, 1968), pp. 188–190.

[20] The integrand diverges at $x' = 1/2$, but the integral converges when the upper limit of integral approaches 1/2 from below.

[21] J. Nenonen and T. Katila, in *Biomagnetism '87*, edited by K. Atsumi, M. Kotani, S. Ueno, T. Katila, and S. J. Williamson (Denki U. P., Tokyo, 1988), p. 426.

[22] See their Eq. (45) and an expression in the following paragraph.

[23] See their Eq. (5) in the case $d \gg t$.

[24] This is the case after correcting the definition of ζ^2 by multiplying it with z^2 in order to render it dimensionless as claimed.